JOURNAL OF VIROLOGY, Dec. 2011, p. 12160–12169 Vol. 85, No. 23
0022-538X/11/$12.00 doi:10.1128/JVI.05703-11


# Vesicular Stomatitis Virus Oncolytic Treatment Interferes with Tumor-Associated Dendritic Cell Functions and Abrogates Tumor Antigen Presentation▽

Simon Leveille,[1,2]† Marie-Line Goulet,[1]† Brian D. Lichty,[3] and John Hiscott[1,2,4]*

*Lady Davis Institute for Medical Research, Jewish General Hospital, Montreal, Quebec, Canada[1]; Departments of Microbiology & Immunology and Medicine, McGill University, Montreal, Quebec, Canada[2]; Center for Gene Therapeutics, Department of Pathology & Molecular Medicine, McMaster University, Hamilton, Ontario, Canada[3]; and Vaccine & Gene Therapy Institute of Florida, Port St. Lucie, Florida 34987[4]*

Received 18 July 2011/Accepted 7 September 2011

**Oncolytic virotherapy is a promising biological approach to cancer treatment that contributes to tumor eradication via immune- and non-immune-mediated mechanisms. One of the remaining challenges for these experimental therapies is the necessity to develop a durable adaptive immune response against the tumor. Vesicular stomatitis virus (VSV) is a prototypical oncolytic virus (OV) that exemplifies the multiple mechanisms of oncolysis, including direct cell lysis, cellular hypoxia resulting from the shutdown of tumor vasculature, and inflammatory cytokine release. Despite these properties, the generation of sustained antitumor immunity is observed only when VSV is engineered to express a tumor antigen directly. In the present study, we sought to increase the number of tumor-associated dendritic cells (DC) *in vivo* and tumor antigen presentation by combining VSV treatment with recombinant Fms-like tyrosine kinase 3 ligand (rFlt3L), a growth factor promoting the differentiation and proliferation of DC. The combination of VSV oncolysis and rFLt3L improved animal survival in two different tumor models, i.e., VSV-resistant B16 melanoma and VSV-sensitive E.G7 T lymphoma; however, increased survival was independent of the adaptive CD8 T cell response. Tumor-associated DC were actively infected by VSV *in vivo*, which reduced their viability and prevented their migration to the draining lymph nodes to prime a tumor-specific CD8 T cell response. These results demonstrate that VSV interferes with tumor DC functions and blocks tumor antigen presentation.**

Cancer therapy using oncolytic viruses (OV) has achieved remarkable therapeutic effects in numerous preclinical tumor models and clinical trials (4, 30). Of the different OV currently evaluated for efficacy, vesicular stomatitis virus (VSV) has emerged as a prototypical OV based on properties such as cancer cell tropism, cell lysis efficacy, and sensitivity to host antiviral responses (3, 24, 33). Tumor regression induced by VSV oncolysis is a complex event that is not limited to direct cell killing by virus infection; cellular hypoxia resulting from the shutdown of tumor vasculature also cooperates to reduce tumor burden (7, 8). Moreover, the innate immune response and accompanying inflammatory cytokine release contribute to the therapeutic effect observed in various murine models (18, 28, 36).

VSV oncolytic therapy has also been proposed to induce a tumor-specific adaptive immune response because infection and concomitant cell lysis expose tumor antigens within a pro-inflammatory milieu. Early studies demonstrated the presence of tumor-specific CD8 T cells following VSV treatment and a reduction of the therapeutic effect after CD8 T cell depletion (15). However, subsequent studies indicated that tumor-specific CD8 T cells either were not detected in the tumor, spleen, or draining lymph nodes following VSV treatment (35) or were detected at low levels that were not statistically significant (9, 10, 17, 37). It was also suggested that tumor regression in CD8 T cell depletion experiments was the result of nonspecific CD8 T cell activation induced by VSV rather than a tumor-specific response (17, 35). Furthermore, VSV treatment did not lead to significant gamma interferon (IFN-γ) secretion in tumor-specific CD8 T cells, even when tumor-specific T cells were adoptively transferred (15, 37). In fact, antitumor immunity following VSV oncolytic treatment has been successfully generated only when VSV was engineered to directly express a tumor antigen (9, 10, 15, 21, 37). Altogether, these studies argue that effector T cell functions remain intact during VSV oncolysis but indicate that antigen presentation may be a limiting step in the initiation of a tumor-specific adaptive immune response.

Dendritic cells (DC) are the most potent antigen-presenting cells and represent the main cell subset capable of cross-presenting tumor antigens in association with major histocompatibility complex (MHC) class I molecules. Several immunotherapy strategies have targeted DC to break tumor tolerance and prime tumor immune responses (19, 27, 32); however, in the context of oncolytic virotherapy, studies on the interaction of VSV and DC remain limited. VSV has been shown to induce the maturation of bone marrow-derived dendritic cells (BMDC) *in vitro*, and infected BMDC were successfully used as cell carriers for VSV oncolytic therapy (1, 2, 5). However, the effect of VSV oncolytic treatment on DC functions *in vivo* has not been studied in detail.

We hypothesized that robust tumor antigen presentation

* Corresponding author. Mailing address: Vaccine & Gene Therapy Institute of Florida, 11350 S.W. Village Parkway, Port St. Lucie, FL 34987. Phone: (772) 345-4768. Fax: (772) 345-3675. E-mail: jhiscott@vgtifl.org.

† S.L. and M.-L.G. contributed equally to this work.

▽ Published ahead of print on 14 September 2011.

may be the missing link required to mount an antitumor adaptive immune response following VSV oncolytic therapy. To boost the antigen presentation capacity during VSV oncolysis *in vivo*, the number of tumor-associated DC was increased by using recombinant Fms-like tyrosine kinase 3 ligand (rFlt3L), a growth factor promoting the differentiation and proliferation of DC (26). In the present study, we demonstrate that the combination of VSV oncolysis and rFLt3L improved animal survival in two different tumor models, i.e., VSV-resistant B16 melanoma and VSV-sensitive E.G7 T lymphoma. Although rFlt3L treatment did increase tumor antigen presentation, VSV abrogated this effect by infecting tumor DC, resulting in the failure of DC to migrate to draining lymph nodes to prime a tumor-specific CD8 T cell immune response.

## MATERIALS AND METHODS

**Cells.** B16 cells expressing ovalbumin (referred to as B16 here) were a kind gift from RG Vile (Mayo Clinic, Rochester, MN) and were grown in Dulbecco modified Eagle medium (DMEM) with 10% fetal bovine serum (FBS) and 5 mg/ml G418. E.G7 cells were provided by J. Galipeau (McGill University, Montreal, Canada) and were grown in RPMI with 10% FBS and 0.5 mg/ml G418. TSA mammary adenocarcinoma cells were provided by G. Barber (University of Miami, Miami, FL) and grown in RPMI with 10% FBS. B16-F1 cells [referred to as B16(Native)] were obtained from ATCC (Manassas, VA) and cultured as recommended. BMDC were differentiated as previously described (20) with 10 ng/ml of mouse granulocyte-macrophage colony-stimulating factor (GM-CSF) and interleukin-4 (IL-4) (R&D Systems, Minneapolis, MN) for 6 days and were typically >85% $CD11c^+$. Where indicated, cells were treated with 1 μg/ml of lipopolysaccharide (LPS) (Sigma, St. Louis, MO) and/or 5 μg/ml SIINFEKEL peptide for the last 24 h.

**Viruses and construction of recombinant VSV.** All VSVs harbor the methionine 51 deletion in the matrix protein-coding sequence (33). The soluble form of the human Flt3L gene was amplified from pUMVC3-hFlex (Aldevron, Fargo, ND) and cloned between the G and L genes. Infectious recombinant VSV was recovered as previously described (22) and replicated as efficiently as parental VSV. VSV-green fluorescent protein (GFP) was kindly provided by J. Bell (Ottawa Health Research Institute). Virus stocks were grown in Vero cells, concentrated from cell-free supernatants by centrifugation, and titrated by standard plaque assay.

**Tumor models and VSV treatment.** C57BL/6 (Thy1.2) and BALB/c mice were purchased from Charles River (Wilmington, MA), and C57BL/6 (Thy1.1) and OT1 (C57BL/6; Thy1.2) mice were purchased from Jackson Laboratory (Bar Harbor, ME). E.G7 ($3 \times 10^6$), B16 ($1 \times 10^6$), or TSA ($3 \times 10^5$) cells were injected subcutaneously (s.c.) in the flanks of 8- to 10-week-old syngeneic female; at 7 days postinoculation, two intratumoral injections of VSV were given on days 0 and 3 ($2 \times 10^7$ PFU for E.G7 and TSA and $2 \times 10^8$ PFU for B16). rFlt3L, kindly provided by Celldex Therapeutics (Phillipsburg, NJ), was administered s.c. in the nape of the neck (10 μg/day) for 10 days starting 8 days before the first VSV injection (26). Tumor volumes were calculated using the formula length × $width^2/2$, and mice were sacrificed when tumor volumes reached 2,000 $mm^3$. All animal experimentations were approved by the McGill University Animal Care Committee.

***In vivo* assays and flow cytometry analysis.** Blood leukocyte counts were obtained using a Vet ABC hematology analyzer (SCIL, Gurnee, IL). Tumor draining lymph nodes refer to both inguinal and axillary lymph nodes. Cell suspensions were prepared by straining through a 70-μm nylon cell strainer (BD Falcon). Total counts were obtained using a Z2 counter (Beckman Coulter, Brea, CA) and multiplied by the proportion obtained by flow cytometry to obtain absolute counts. B16 tumors were weighted, strained through a 100-μm nylon cell strainer (BD Falcon), and resuspended at 20% (wt/vol) to stain comparable numbers of cells for flow cytometry. Absolute numbers of tumor cell populations were determined using Sphero AccuCount fluorescent beads (Spherotech, Lake Forest, IL) as per the manufacturer's instructions. Briefly, cells were treated with Fc Block (BD Biosciences), incubated with antibodies, washed once, and resuspended in 1 ml; 50 μl of counting beads was added and vortexed just prior to acquisition. Populations in Fig. 4 were gated as follow: total leukocytes, $CD45^+$; neutrophils, $CD45^+$ $CD11b^+$ $Gr1^+$ $F4/80^-$; myeloid-derived suppressor cells (MDSC), $CD45^+$ $CD11b^+$ $Gr1^+$ $F4/80^+$; macrophages, $CD45^+$ $F4/80^+$ $Gr1^-$; DC, $CD45^+$ $CD11c^+$ $NK1.1^-$; CD4 T cells, $CD45^+$ $CD3^+$ $CD4^+$ $CD8^-$; CD8 T cells, $CD45^+$ $CD3^+$ $CD8^+$ $CD4^-$; and NK cells, $CD45^+$ $CD11c^-$ $NK1.1^+$. B cells ($CD45R^+$) were not significantly represented in the tumor, and plasmacytoid DC (pDC) could not be reliably analyzed. E.G7 and TSA tumors were digested with collagenase IV and DNase I (Sigma-Aldrich, St. Louis, MO). All antibodies were purchased from eBioscience (San Diego, CA) unless indicated otherwise. Samples were acquired on a FACSCalibur (BD Biosciences) and analyzed with FCS Express 3 (De Novo Software, Los Angeles, CA).

***Ex Vivo* peptide restimulation.** Cells ($2 \times 10^6$) were incubated with 5 μg/ml of peptide and 2 μg/ml of CD28 antibody (BD Biosciences) for 5 h. GolgiPlug (BD Biosciences) was added after 1 h, and IFN-γ (BD Biosciences) intracellular staining was performed using the BD Cytofix/Cytoperm kit as per the manufacturer's instructions. SIINFEKL (ovalbumin [OVA]), RGYVYQSL (VSV N), and DAPIYTNV (irrelevant [β-galactosidase]) peptides were produced by the Sheldon Biotechnology Center (McGill University, Montreal, Canada). For positive control of the OVA-specific response, $2.5 \times 10^6$ LPS-matured BMDC pulsed with SIINFEKEL were injected intraperitoneally (i.p.).

**OT1 proliferation assays.** CD8 OT1 T cells (Thy1.2) were isolated using a CD8 T cell enrichment kit (Stemcell, Vancouver, BC, Canada) and labeled with 5 μM carboxyfluorescein succinimidyl ester (CFSE). For *in vivo* proliferation, $3 \times 10^6$ OT1 cells were injected intravenously (i.v.) into C57BL/6 (Thy1.1) mice at 24 h after the first dose of VSV. CFSE dilution was analyzed by fluorescence-activated cell sorting (FACS) 6 days later. For *in vitro* proliferation, draining lymph node DC were isolated from C57BL/6 (Thy1.2) mice at 24 h following VSV treatment using a CD11c positive selection kit (Stemcell) and incubated with OT1 T cells at a 2:1 ratio for 3 days.

***In vivo* migration assays.** For DC migration, LPS-matured BMDC were labeled with 5 μM CFSE (Invitrogen, Carlsbad, CA), and $1.5 \times 10^6$ cells were injected intratumorally in B16 tumors. Upregulation of CCR7 by LPS was confirmed by FACS. For lymphocyte migration, tumor lymphocytes were isolated from 7-day-old B16 tumors growing in C57BL/6 (Thy1.1) mice by using a Ficoll gradient (GE Healthcare, United Kingdom) and reinjected intratumorally into C57BL/6 (Thy1.2) mice bearing 7-day-old B16 tumors. Cells isolated from a certain number of tumors were reinjected into the same number of tumors. Cell migration was evaluated at 40 h following treatment.

**DC infection and viability.** The analysis was performed at 10 h following VSV injection prior to DC loss from the tumor. B16 tumors were stained with anti-CD45 and -CD11c antibodies, and GFP was analyzed by FACS. DC were analyzed as $CD45^+$ $CD11c^{Hi}$ and tumors as $CD45^-$. For determination of *in vivo* tumor DC viability, B16 tumors were gently dispersed by pipetting and stained with CD11c, annexin V, and propidium iodide (PI) for FACS analysis. For determination of *in vitro* infectivity, BMDC were infected with VSV in a small volume of medium without FBS for 1 h; cells were then incubated in complete medium containing 10 ng/ml GM-CSF and IL-4. Cell viability was assessed using annexin V (BD) and PI (Sigma-Aldrich, St. Louis, MO) by FACS or by direct counting using trypan blue.

**Statistical analysis.** Unpaired *t* test and log rank statistical analyses were performed using Prism 4 (GraphPad, San Diego, CA). The error bars in the figures represent standard errors of the means (SEM).

## RESULTS

**Increasing the number of dendritic cells using rFlt3L improves animal survival.** A strategy was designed to combine VSV and rFlt3L to enhance tumor antigen presentation during VSV oncolysis. The combination approach was evaluated *in vivo* in two different subcutaneous tumor models expressing ovalbumin (OVA) as a model tumor antigen: the B16 melanoma model is relatively resistant to VSV oncolysis, and high intratumoral doses of virus ($2 \times 10^8$ PFU) are required to inhibit tumor growth (reference 18 and data not shown); in contrast, the E.G7 T lymphoma model is sensitive to VSV, and tumors are cured by VSV at $\sim 1 \times 10^7$ PFU (data not shown). As previously reported (26), daily administration of rFlt3L increased DC numbers in the blood and lymphoid organs at 9 to 10 days following treatment; moreover, DC infiltrated the tumor mass with similar kinetics, resulting in a 4-fold increase in tumor DC at day 9 after treatment (Fig. 1a). To optimize the presentation of tumor antigens, rFlt3L injections were over-

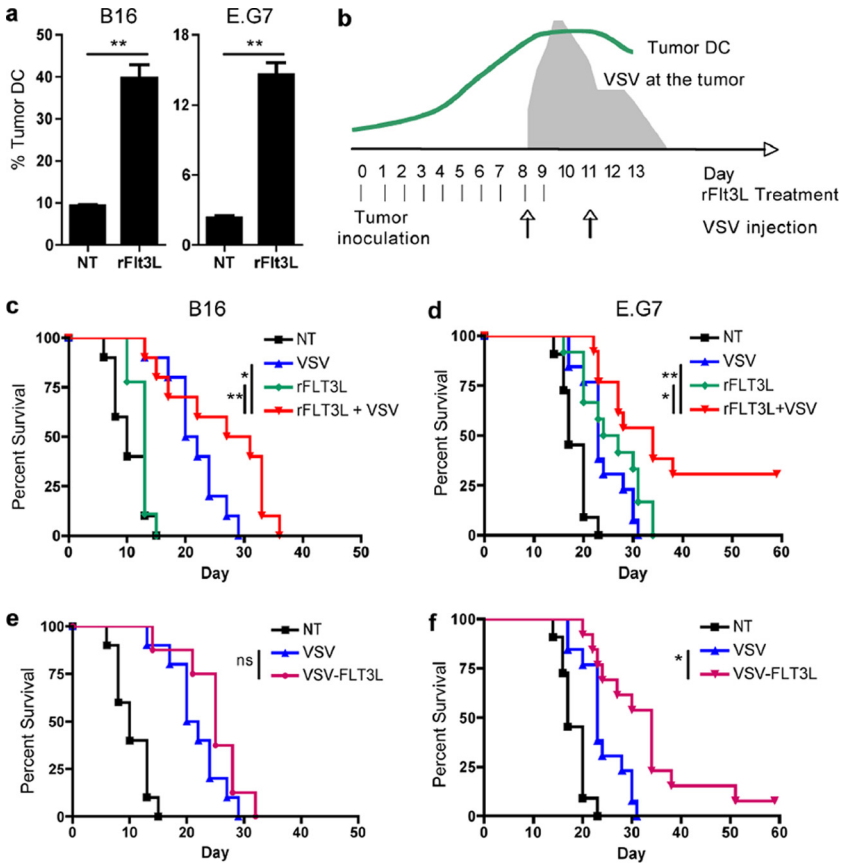


FIG. 1. The combination of VSV and Flt3L improves animal survival. (a) Tumor DC were evaluated by flow cytometry after 9 days of rFlt3L treatment, and the data are presented as the percentage of $CD11c^+$ cells per $CD45^+$ cells (B16) or per total cells (E.G7). (b) Schematic representation of the different treatment regimens. rFlt3L was administrated daily for 10 days starting 8 days before the first dose of VSV. Animals received two additional intratumoral VSV injections 3 days apart. (c to f) B16 (c and e) or E.G7 (d and f) tumor-bearing mice were treated with either rFlt3L, VSV, rFlt3L and VSV, or VSV-FLT3L or nontreated (NT), and survival was monitored (B16 [$n = 10$] and EG7 [$n = 13$]). *, $P < 0.05$; **, $P < 0.005$; ns, not significant.

lapped with VSV infections so that the peak number of tumor DC coincided with maximal tumor cell lysis and antigen release, which occur at 24 to 48 h following the initial injection of VSV (18, 23) (Fig. 1b). While treatment of animals with rFlt3L alone had no effect in the B16 tumor model, the combination of rFlt3L with VSV treatment significantly improved animal survival (Fig. 1c). Because of the sensitivity of E.G7 to VSV, the efficacy of the combination in this model was evaluated in a distant nontreated E.G7 tumor on the opposite flank, such that animal survival was dictated by a therapeutic immune response in the distant tumor. VSV as a single treatment led to a minor delay in the growth of the distant tumor early after treatment (Fig. 1d). Similarly, rFlt3L treatment improved animal survival, indicating that the E.G7 tumor model was partially sensitive to the effects of rFlt3L (Fig. 1d). Nevertheless, the combination of VSV with rFlt3L significantly improved animal survival and completely cured approximately 30% of animals (Fig. 1d). Therefore, rFlt3L treatment augmented the number of DC prior to VSV treatment and statistically improved animal survival in two different tumor models.

As a second strategy to augment DC, VSV was engineered to express Flt3L directly. The gene insertion did not affect viral replication efficiency, and expression of Flt3L was confirmed by enzyme-linked immunosorbent assay (ELISA) (data not shown). In the B16 model, recombinant VSV-Flt3L did not provide a significant survival advantage compared to parental VSV (Fig. 1e), whereas VSV-Flt3L modestly improved survival in the E.G7 model (Fig. 1f). VSV is present at the tumor for only a few days (18, 23), which correlated with detectable levels of Flt3L in the sera of treated animals for less than 6 days (data not shown). Given that rFlt3L has been shown to augment circulating DC in humans and mice after 8 to 10 days of continuous treatment (26), VSV-Flt3L expression may be not sustained for a sufficient time to reproduce the survival advantage observed with rFlt3L.

**The efficacy of the VSV and rFlt3L combination is independent of the adaptive CD8 T cell response.** The combination of VSV oncolysis and rFlt3L was intended to increase tumor antigen presentation and favor a tumor-specific adaptive immune response. Therefore, the specificity of CD8 T cells for tumor or viral antigen was monitored in tumor draining lymph nodes 10 days after VSV injection by restimulating lymphocytes with either an OVA or a VSV peptide, followed by IFN-γ quantification by flow cytometry. In both the B16 and the E.G7 tumor models, VSV treatment induced a strong antiviral response (Fig. 2a and b). However, as previously reported (10,

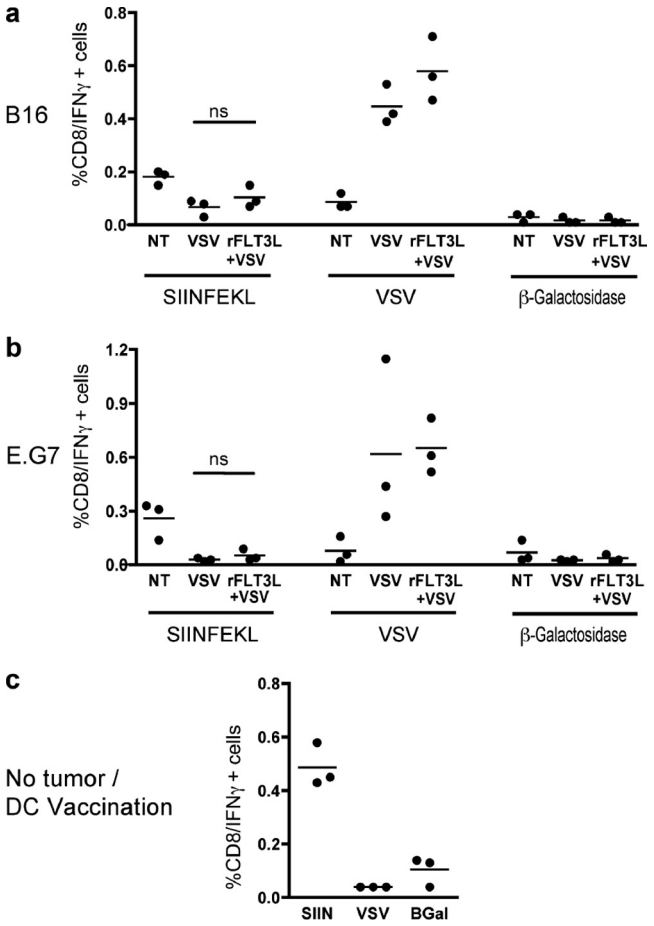


FIG. 2. The VSV and rFtl3L combination does not improve the tumor-specific CD8 T cell response. (a and b) B16 (a) or E.G7 (b) tumors were injected into one flank with VSV; at 10 days following the first dose of VSV, draining lymph nodes were harvested and $CD8^+$ $CD11c^-$ T lymphocytes specific for tumor SIINFEKL or VSV N peptides were monitored using *ex vivo* peptide restimulation followed by IFN-γ intracellular staining. (c) As a positive control, mice were injected i.p. with bone marrow-derived dendritic cells, pulsed with SIIN FEKL, and analyzed in parallel at 10 days following vaccination. β-Galactosidase peptide was used as a negative control. ns, not significant.

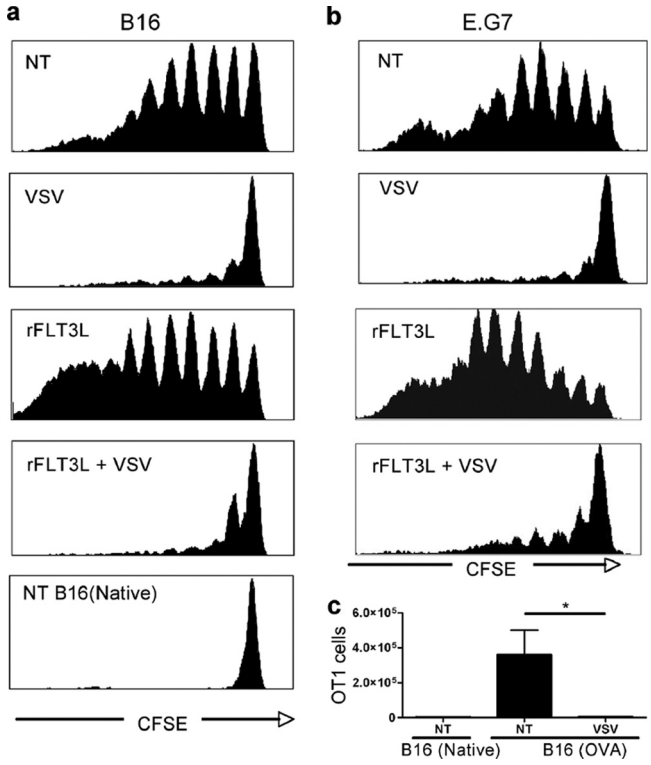


FIG. 3. VSV infection abrogates antigen presentation by DC. (a and b) B16(OVA) or B16(Native) (a) or E.G7 (b) tumor-bearing mice (Thy1.1) were injected i.v. with CFSE-labeled OT1 CD8 T cells (Thy1.2) at 24 h after the first VSV injection. At 6 days after adoptive transfer, tumor draining lymph nodes were collected and CFSE dilution in $Thy1.2^+$ cells was monitored by FACS. (c) Tumors from animals used for panel a were analyzed by FACS to identify effector Thy1.2+ OT-1 T cells ($n = 3$). *, $P < 0.05$.

35), VSV alone did not generate a significant CD8 T cell response against SIINFEKL compared to the antiviral response (Fig. 2a and b) or to the vaccination with mature bone-marrow derived dendritic cells (BMDC) pulsed with SIIN FEKL peptide (Fig. 2c). In fact, fewer T cells were detected following VSV treatment than in untreated animals. Following combination treatment, the proportion of IFN-γ-producing CD8 T cells specific for the SIINFEKL peptide was not increased (Fig. 2a and b), a result that was further confirmed via SIINFEKL-tetramer staining (data not shown). Thus, the improved survival rate observed with the combination therapy cannot be attributed to the generation of a tumor-specific CD8 T cell response.

**VSV infection abrogates tumor antigen presentation.** To investigate why augmenting DC did not favor an adaptive immune response, the effect of rFlt3L treatment and VSV oncolysis on tumor antigen presentation was analyzed *in vivo*. OT-1 CD8 T cells specific for SIINFEKL were adoptively transferred to tumor-bearing animals, and their proliferation in response to antigen presentation was traced through CFSE dilution in the tumor draining lymph nodes. In both tumor models, OVA antigen was constitutively presented in untreated animals (Fig. 3a and b, NT); however, the absence of an inflammatory stimulus likely prevented the generation of a functional adaptive CD8 T cell response (Fig. 2a and b). rFlt3L treatment further increased OT-1 T cell proliferation (Fig. 3a and b, rFlt3L), indicating that the increase in DC number improved tumor antigen presentation. Surprisingly, after VSV treatment, the proliferation of OT-1 T cells was completely arrested in both the B16 and the E.G7 tumor models (Fig. 3a and b, VSV and rFlt3L + VSV). To rule out the possibility that OT-1 T cells had migrated from the lymph nodes to perform effector functions at the tumor site, the tumor was also analyzed. A small number of proliferating OT-1 T cells were detected in the tumors of untreated animals; however, no OT1 T cells were detected in tumors that had received VSV treatment (Fig. 3c). Thus, VSV treatment abrogated tumor antigen presentation *in vivo*, and augmentation of DC using rFlt3L was not sufficient to overcome this block.

**VSV treatment reduces the number of tumor-associated dendritic cells.** Given that VSV treatment abrogated tumor antigen presentation, we next examined the fate of DC during VSV oncolysis. Flow cytometry analysis revealed that VSV

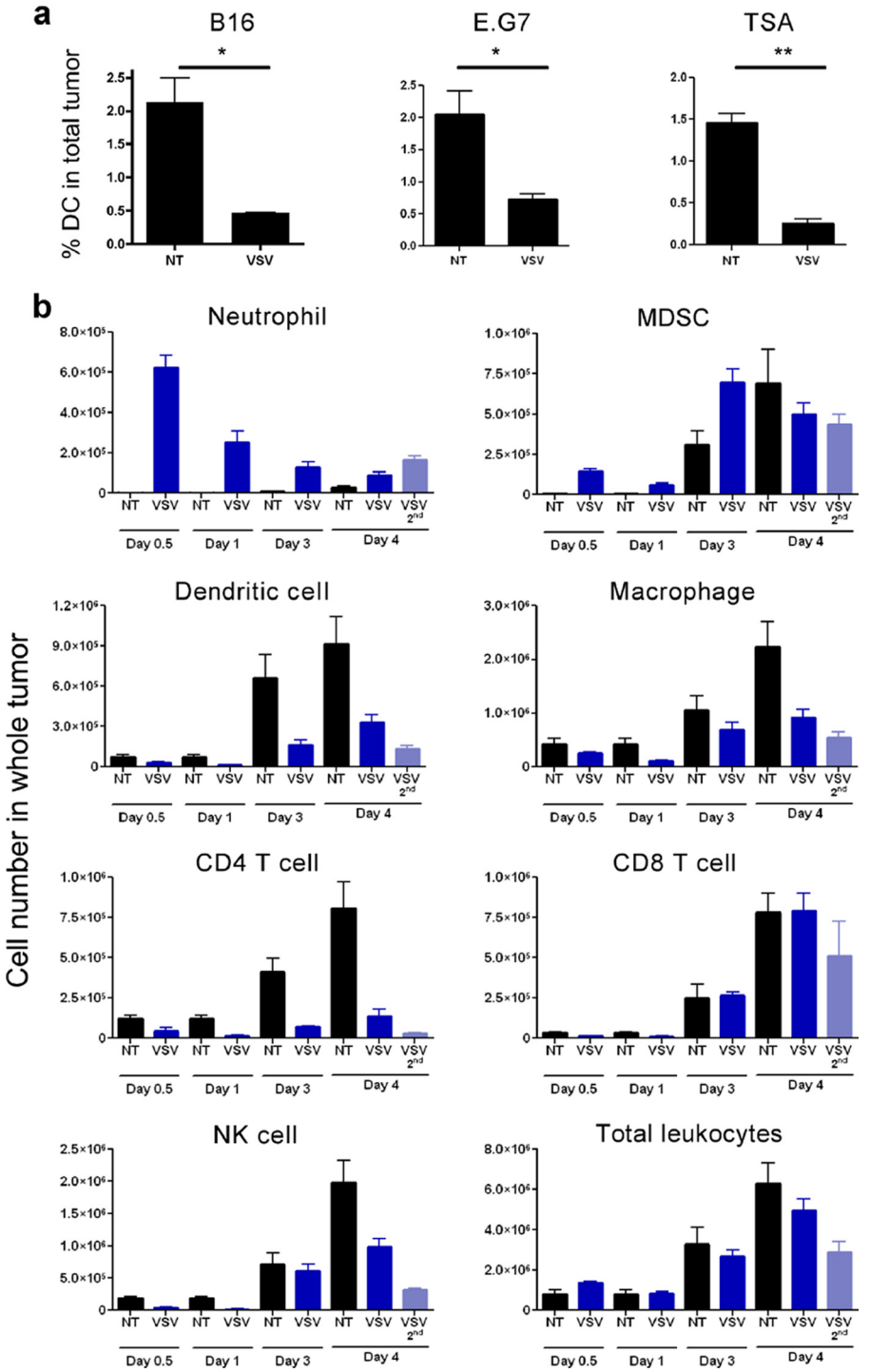


FIG. 4. Tumor DC and tumor leukocytes decrease following VSV treatment. (a) B16, E.G7, or TSA tumors were treated with parental VSV, and the proportion of $CD11c^+$ DC in the tumor cell homogenate was evaluated by FACS at 24 h after injection ($n = 3$). (b) B16 tumors were treated with VSV and collected at time points −12 h, 24 h, 72 h, and 96 h after the first VSV injection, as well as 24 h after the second VSV injection. Cells were stained with different panels of antibodies and enumerated by flow cytometry using counting beads. Data are presented as absolute cell number in whole tumor to account for the neutrophil infiltration that would bias relative proportions ($n = 4$). *, $P < 0.05$; **, $P < 0.005$.

intratumoral injection rapidly decreased the number of tumor DC after treatment (Fig. 4a) rather than recruiting more DC to the site of inflammation. Moreover, the loss of tumor DC was consistent in three tumor models syngeneic to different murine genetic backgrounds.

To expand on the effect of VSV treatment, the immune cell populations infiltrating B16 tumors were analyzed. An extensive but transient infiltration of neutrophils was observed in the tumor shortly after VSV treatment (Fig. 4b); this cell type has been implicated in tumor vasculature shutdown and tumor cell

hypoxia (8). Myeloid derived suppressor cells (MDSC) were also detected within the tumor, although the kinetics of their infiltration was slower than that for neutrophils (Fig. 4b). In contrast, all other populations of leukocytes analyzed (DC, macrophages, NK cells, CD4 T cells, and CD8 T cells) significantly decreased as early as 12 h after VSV injection and remained low for several days. Further confirming this observation, the reduction in cell number was reproduced at 24 h after the second injection of VSV (Fig. 4b, day 4, VSV 2nd), compared to animals that had received only one injection (day 4, VSV). The loss of immune cells following VSV treatment was not reflected in the total number of leukocytes present at the tumor, because substantial numbers of infiltrating neutrophils compensated for the loss (Fig. 4b). Thus, VSV treatment had a profound impact on tumor immune cells, resulting in the recruitment of only neutrophils and MDSC to the tumor and the loss of DC and other leukocyte populations.

**VSV infects tumor DC and decreases their survival.** To examine the possibility that tumor DC were infected by VSV and eliminated from the tumor *in vivo*, VSV-GFP was injected into the B16 tumors and GFP expression was monitored by flow cytometry. Given that viral infection and cell death induce autofluorescence, viral GFP fluorescence was compared to an infection using a VSV that did not express GFP. The shift in GFP fluorescence intensity confirmed that tumor DC were infected by VSV *in vivo* following treatment (Fig. 5a); ~12% of dendritic cells were infected by VSV, compared to ~3% of tumor cells (Fig. 5b). Similar results were observed in the E.G7 tumor model (data not shown).

Next, the impact of VSV treatment on tumor DC viability was assessed *in vivo* by flow cytometry using annexin V and propidium iodide (PI) discrimination of apoptotic/dead cells. Following VSV treatment, the percentage of recovered live tumor DC decreased from ~80% in untreated tumors to ~50% in VSV-treated tumors (Fig. 5c). As additional support, the viability of BMDC was evaluated *in vitro* following VSV infection. Flow cytometry analysis using annexin V/PI (Fig. 5d, dot plots and gate R1) demonstrated that BMDC died following VSV infection, depending on the multiplicity of infection (MOI) and elapsed time. Previous studies demonstrated that BMDC were infected by VSV *in vitro* but that cell viability was not affected (1, 5). This discrepancy can be explained by the flow cytometry analysis that selected a live cell population based on light scatter characteristics or CD11c expression (Fig. 5d, gate R2). Direct cell counting using trypan blue exclusion further confirmed that BMDC were killed following VSV infection (Fig. 5e). Thus, VSV infected and killed tumor DC *in vivo*, as well as BMDC *in vitro*.

**Loss of functions in tumor DC.** Although a portion of the tumor-associated DC were infected and killed following VSV treatment, the loss of DC from the tumor may also result from their migration to the draining lymph nodes. Concomitant with the loss of DC at the tumor, VSV treatment caused an accumulation of leukocytes in the tumor draining lymph nodes (Fig. 6a). The large number of cells recruited to the draining lymph nodes suggested that immune cell migration from the tumor was not the only source of increased lymph node cellularity. Indeed, total blood leukocyte counts drastically decreased upon VSV treatment (Fig. 6a). Moreover, intratumoral VSV treatment induced a systemic inflammation, since contralateral lymph nodes were also inflamed, albeit to a lesser extent than tumor draining lymph nodes (Fig. 6a).

To determine whether tumor DC migrated to the draining lymph nodes, BMDC were matured using LPS, labeled with CFSE, and injected intratumorally at 4 h before or after VSV injection; traceable cells in the draining lymph nodes were then quantified by flow cytometry. Maturation of BMDC is known to upregulate the CCR7 receptor and induce homing to the lymph nodes (29), and as expected, mature BMDC from untreated tumors migrated to the draining lymph nodes (Fig. 6b). However, a 10-fold decrease in migrating cells was observed following VSV infection, indicating that VSV treatment drastically diminished the migration process. Moreover, DC adoptively transferred after VSV injection migrated less efficiently to the draining lymph nodes than DC allowed to migrate for 4 h prior to VSV injection (Fig. 6b).

Using a more physiological approach, tumor infiltrating lymphocytes were isolated by use of Ficoll gradients from tumors growing in Thy1.1 mice and reinjected intratumorally into Thy1.2 mice in physiological numbers. A small number of Thy1.1 tumor lymphocytes spontaneously migrated from the tumor to the draining lymph nodes following transfer, and consistent with Fig. 4, VSV treatment significantly reduced the number of Thy1.1 cells in the tumor (Fig. 6c). However, this decrease was not associated with the migration of Thy1.1 cells from the tumor to the draining lymph nodes (Fig. 6c). Thus, VSV treatment is proinflammatory, as demonstrated by the recruitment of immune cells to lymphoid organs; even so, tumor DC failed to migrate to the tumor draining lymph nodes.

Finally, the effect of inefficient tumor DC migration on tumor antigen presentation was assessed. DC were isolated from tumor draining lymph nodes, and presentation of tumor antigen was evaluated by the ability of DC to induce the proliferation of CFSE-labeled OT1 T cells following coculture. DC isolated from untreated animals induced the proliferation of OT1 T cells following coincubation (Fig. 6d), while VSV treatment arrested OT-1 proliferation. MDSC induced upon VSV treatment were shown previously to interfere with priming of the adaptive immune response (34). To ascertain that a low frequency of MDSC in purified DC preparations did not interfere with OT-1 proliferation, neutralizing antibodies against transforming growth factor β (TGF-β) and IL-10 were supplemented during culture, but they failed to restore OT1 proliferation (data not shown). Therefore, VSV oncolytic treatment prevented efficient presentation of tumor antigen necessary to initiate an adaptive immune response against the tumor.

## DISCUSSION

Tumor oncolysis driven by VSV exemplifies the complex mechanisms associated with tumor regression, where oncolysis is related to direct cell killing, cellular hypoxia resulting from the shutdown of tumor vasculature, and inflammatory cytokine release. One of the remaining challenges in the development of OV therapies for cancer is to develop a sustained, durable adaptive immune response against the tumor. Although VSV oncolytic therapy has been proposed to induce a tumor-specific adaptive immune response, a number of studies indicated that the generation of antitumor immunity was observed only when

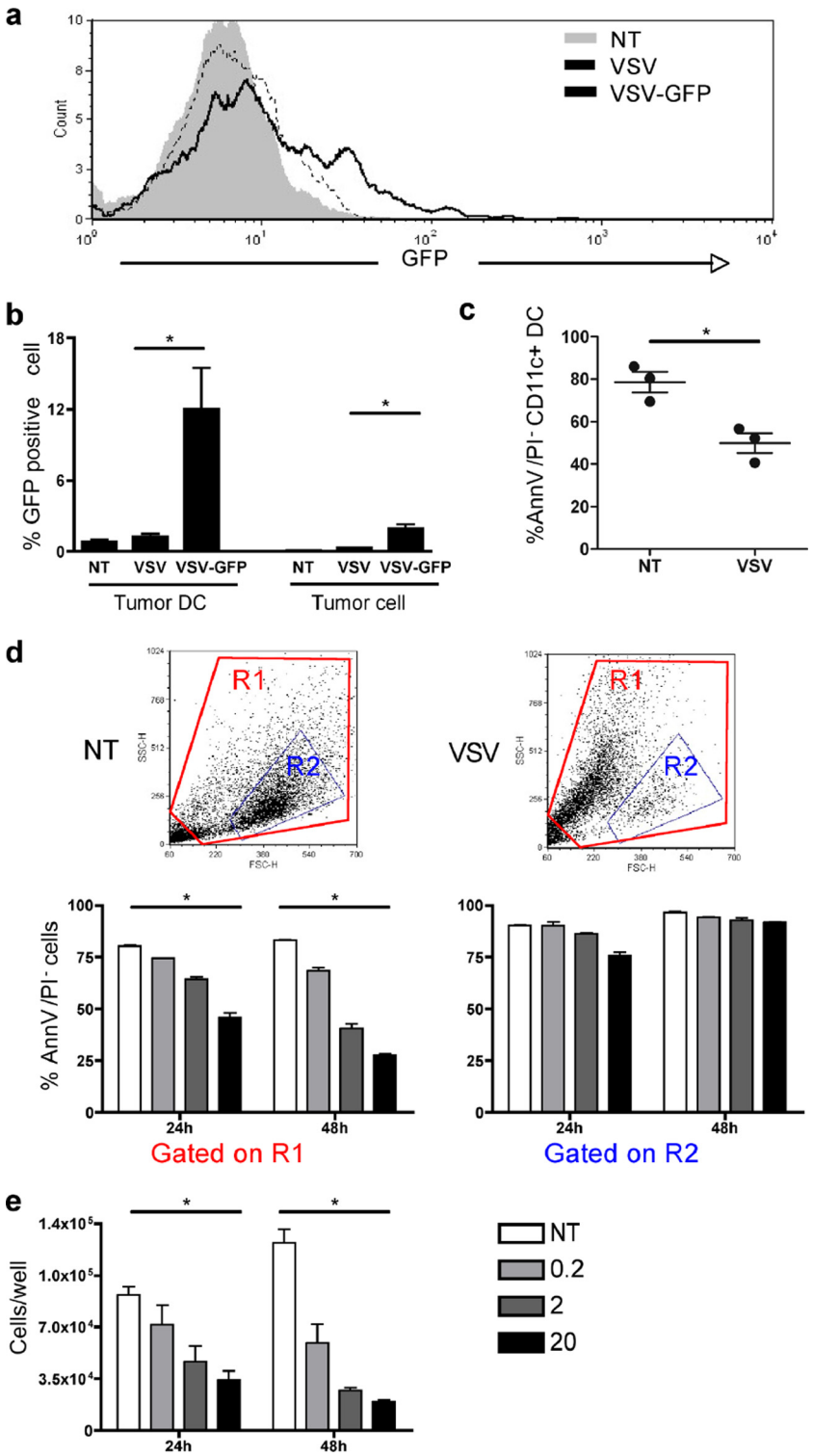


FIG. 5. VSV infection of tumor dendritic cells reduces viability. (a and b) B16 tumors were either left untreated or injected with parental VSV or VSV-GFP. (a) The GFP expression level in $CD11c^+$ tumor DC was analyzed by FACS at 10 h postinjection. (b) The percentage of tumor DC or tumor cells expressing GFP was also analyzed ($n = 3$). Parental VSV without GFP was used as negative control to account for autofluorescence induced upon virus infection. (c) The viability of $CD11c^+$ tumor DC was assessed in B16 tumors at 10 h after VSV injection by annexin V/PI staining ($n = 3$). (d and e) BMDC were infected with VSV-GFP at an MOI of 0.2, 2, or 20, and cell viability was monitored 24 h and 48 h later. (d) FSC/SSC dot plots at 48 h after infection with VSV (MOI of 20) or noninfected (NT). Cell death was assessed using annexin V/PI and analyzed based on region R1 (all events) or region R2 as previously reported (1, 5). (e) Cell death was assessed by live cell counting using trypan blue ($n = 3$). *, $P < 0.05$.

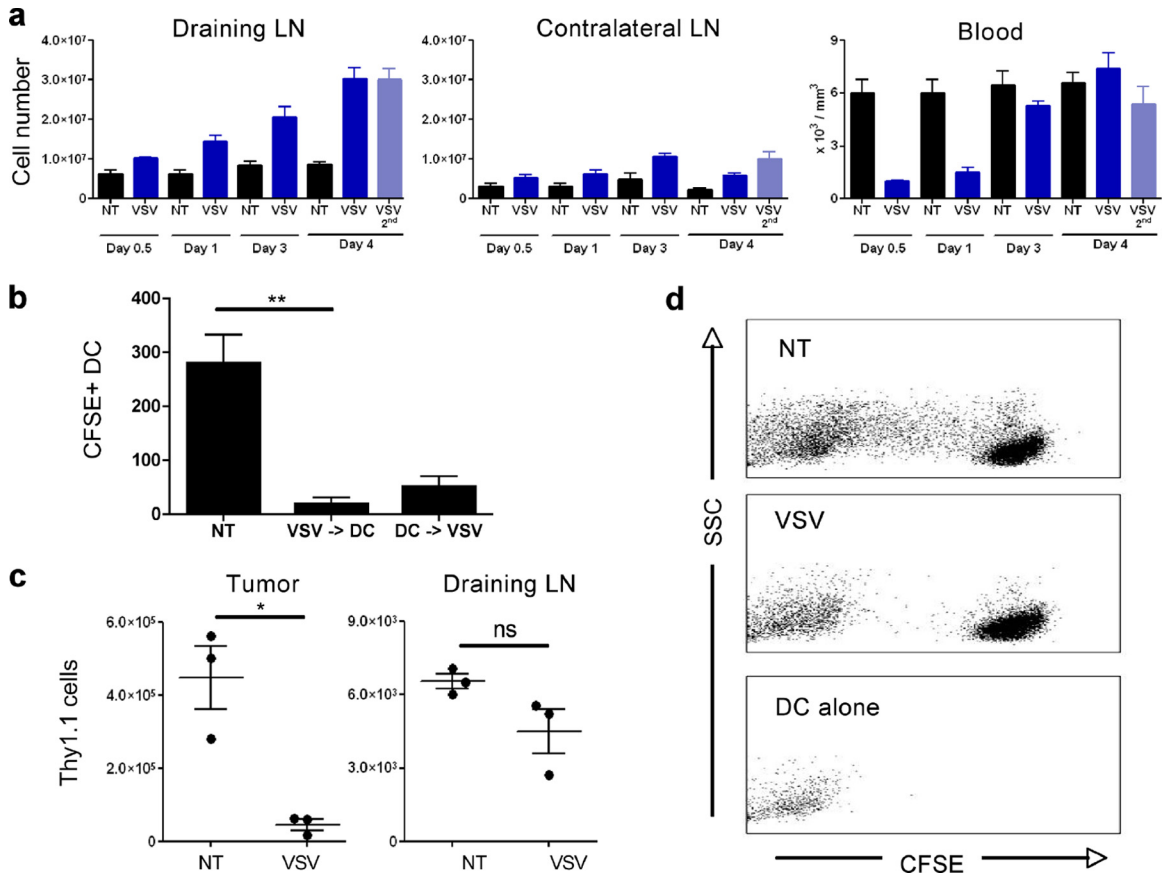


FIG. 6. Tumor DC fail to migrate to the draining lymph nodes after VSV infection. (a) Total leukocyte counts from tumor draining lymph nodes, contralateral lymph nodes, and peripheral blood from B16 tumor-bearing animals at different times following treatment ($n = 4$). (b) LPS-activated BMDC were labeled with CFSE and injected into B16 tumors at 4 h before or after VSV intratumoral injection. At 40 h later $CD11c^+$ $CFSE^+$ DC in draining lymph nodes were measured by FACS ($n = 4$). (c) B16 tumor lymphocytes were isolated by use of Ficoll gradients from Thy1.1 mice and adoptively transferred by intratumoral injection into identical B16 tumors in Thy1.2 mice; VSV was injected 4 h after adoptive transfer. Tumors and draining lymph nodes were collected 40 h later, and $Thy1.1^+$ cells were monitored by FACS. (d) DC were isolated from B16 tumor draining lymph nodes at 24 h after VSV treatment and cocultured with CFSE-labeled OT1 T cells, and CFSE dilution in $CD8^+$ cells was assessed by FACS. Fluorescence of DC is presented as a reference for fluorescence from non-OT1 cells. *, $P < 0.05$; **, $P < 0.005$; ns, not significant.

VSV was engineered to express a tumor antigen directly (9, 10, 15, 21, 37).

In the present study, we sought to increase the number of tumor-associated dendritic cells *in vivo* with the goal to boost tumor antigen presentation and bypass the necessity for viral expression of tumor antigens. The combination of VSV oncolysis and rFLt3L improved animal survival in two different tumor models, i.e., VSV-resistant B16 melanoma and VSV-sensitive E.G7 T lymphoma; however, increased survival was independent of the adaptive CD8 T cell response. rFlt3L treatment increased tumor antigen presentation, but VSV oncolysis abrogated this effect by inducing the rapid disappearance of tumor-associated DC. VSV treatment led to the infection and killing of tumor DC *in vivo*, thus preventing their migration to the lymphoid organs to initiate an antigen-specific immune response. Our results showing the inhibition of antigen presentation to tumor-specific CD8 T cells differ from an earlier report describing the proliferation of OT1 T cells in the tumor draining lymph nodes following VSV-GFP treatment (15); however, a recent study demonstrated that the percentage of adoptively transferred OT1 T cells in the tumor draining lymph nodes was actually lower following VSV-GFP treatment than in control animals (37). Consistent with the latter observation, VSV oncolysis did not activate OT1 T cells and did not lead to tumor infiltration by OT1 T cells (Fig. 3) (15, 37), thus supporting the observation that VSV interferes with tumor antigen presentation.

Dendritic cells are the most efficient antigen-presenting cells and function as the link between innate and adaptive immunity. The immunological paradigm is that DC capture antigens, while inflammatory signals trigger their maturation and migration to the draining lymph nodes to initiate an antigen-specific immune response (19, 32). As previously described *in vitro* for BMDC (1, 2, 5), we observed that VSV infection induced the maturation of tumor DC *in vivo* through the upregulation of different costimulatory molecules (S. Leveille and M.-L. Goulet, unpublished observation). Hence, VSV has the capacity to convert immature tolerogenic DC into mature cells capable of priming T cells; however, the present results revealed that VSV infection prevented the generation of a T cell response against

the tumor, even when the number of DC was increased by pre treatment with rFlt3L. Although VSV interfered with tumor dendritic cell functions and prevented a tumor-specific adaptive immune response, a strong antiviral response was mounted following VSV treatment. DC have been shown to play a crucial role in priming anti-VSV immune responses (11–13, 25). Recently, the dissemination of highly immunogenic viral particles to the tumor draining lymph nodes shortly after intratumoral injection was reported (37). Infection of resident lymph node DC by recombinant VSV expressing OVA was proposed to be responsible for the OVA-specific immune response (37), thus implying that the antiviral response depends on lymph node DC rather than tumor DC.

Variability in the percentage of apoptotic DC was observed in the *in vivo* assays, and we suspect that the extent of DC killing may be underestimated, given the rapid clearance of apoptotic cells, the loss of dead cells during sample processing, and the loss of lineage markers upon cell death. The ability of VSV to infect and kill DC *in vivo* was also tested in an *in vitro* setting, where we showed that BMDC were also infected and killed by VSV. Factors other than direct viral infection may also contribute to tumor DC cell death. For example, deficiency in blood flow resulting from tumor vascular shutdown could induce tumor DC death by hypoxia, as reported for noninfected tumor cells (8). This blockage of vascularization could also confine cells to a microenvironment that favors prolonged exposure to virus and thus increases cell susceptibility to infection.

The combination of VSV and rFLT3L treatment improved survival of the animals through a mechanism independent of the CD8 T cell response. Flt3L, in addition to increasing the number of conventional myeloid DC, acts as a growth factor for plasmacytoid DC and NK cells (26, 31). Increasing the number of plasmacytoid DC, which are a major interferon (IFN)-producing cell type, would likely enhance the local production of type I IFN upon VSV infection, thus contributing to the therapeutic effect of VSV treatment (36). Furthermore, the expansion of NK cells is suggestive of an enhanced NK cell-mediated tumor cytotoxicity and cross talk with abundant DC (6, 14, 16). Thus, although designed to improve the antitumor adaptive immune response, the combination of Flt3L with VSV may further benefit the innate immune response against the tumor.

In conclusion, the results presented here describe a mechanism that explains the limited capacity of VSV to trigger a tumor-specific adaptive immune response. Integrating these findings into the rational design of new VSV-based cancer immunotherapy will be a major step toward complementing the acute oncolytic properties of VSV with long-lasting tumor immunity. Such an approach was described recently, in which a cDNA library from normal prostate tissue was expressed in the context of VSV (21). Prostate tumors of the same histological type from which the cDNA library was derived were cured when challenged with prostate antigen expressing VSV. This approach permitted systemic delivery and presentation of a broad repertoire of tumor-associated antigens (21) and circumvented the limitations of antigen presentation associated with oncolytic approaches for cancer therapy.

## ACKNOWLEDGMENTS

This research was supported by grants to J.H. from the Terry Fox Foundation, the Canadian Cancer Society (CCS), and the Canadian Institutes of Health Research. S.L. was supported by a studentship from the National Science and Engineering Council.

## REFERENCES

1. **Ahmed, M., K. L. Brzoza, and E. M. Hiltbold.** 2006. Matrix protein mutant of vesicular stomatitis virus stimulates maturation of myeloid dendritic cells. J. Virol. **80:**2194–2205.
2. **Ahmed, M., et al.** 2009. Vesicular stomatitis virus M protein mutant stimulates maturation of Toll-like receptor 7 (TLR7)-positive dendritic cells through TLR-dependent and -independent mechanisms. J. Virol. **83:**2962–2975.
3. **Barber, G. N.** 2005. VSV-tumor selective replication and protein translation. Oncogene **24:**7710–7719.
4. **Bell, J.** 2010. Oncolytic viruses: an approved product on the horizon? Mol. Ther. **18:**233–234.
5. **Boudreau, J. E., et al.** 2009. Recombinant vesicular stomatitis virus transduction of dendritic cells enhances their ability to prime innate and adaptive antitumor immunity. Mol. Ther. **17:**1465–1472.
6. **Boudreau, J. E., et al.** 2011. IL-15 and type I interferon are required for activation of tumoricidal NK cells by virus-infected dendritic cells. Cancer Res. **71:**2497–2506.
7. **Breitbach, C. J., et al.** 2011. Targeting tumor vasculature with an oncolytic virus. Mol. Ther. **19:**886–894.
8. **Breitbach, C. J., et al.** 2007. Targeted inflammation during oncolytic virus therapy severely compromises tumor blood flow. Mol. Ther. **15:**1686–1693.
9. **Bridle, B. W., et al.** 2009. Vesicular stomatitis virus as a novel cancer vaccine vector to prime antitumor immunity amenable to rapid boosting with adenovirus. Mol. Ther. **17:**1814–1821.
10. **Bridle, B. W., et al.** 2010. Potentiating cancer immunotherapy using an oncolytic virus. Mol. Ther. **18:**1430–1439.
11. **Ciavarra, R. P., et al.** 2000. Antigen processing of vesicular stomatitis virus in situ. Interdigitating dendritic cells present viral antigens independent of marginal dendritic cells but fail to prime CD4(+) and CD8(+) T cells. Immunology **101:**512–520.
12. **Ciavarra, R. P., A. Stephens, S. Nagy, M. Sekellick, and C. Steel.** 2006. Evaluation of immunological paradigms in a virus model: are dendritic cells critical for antiviral immunity and viral clearance? J. Immunol. **177:**492–500.
13. **Ciavarra, R. P., et al.** 2005. Impact of macrophage and dendritic cell subset elimination on antiviral immunity, viral clearance and production of type 1 interferon. Virology **342:**177–189.
14. **Degli-Esposti, M. A., and M. J. Smyth.** 2005. Close encounters of different kinds: dendritic cells and NK cells take centre stage. Nat. Rev. Immunol. **5:**112–124.
15. **Diaz, R. M., et al.** 2007. Oncolytic immunovirotherapy for melanoma using vesicular stomatitis virus. Cancer Res. **67:**2840–2848.
16. **Fernandez, N. C., et al.** 1999. Dendritic cells directly trigger NK cell functions: cross-talk relevant in innate anti-tumor immune responses in vivo. Nat. Med. **5:**405–411.
17. **Galivo, F., et al.** 2010. Interference of CD40L-mediated tumor immunotherapy by oncolytic vesicular stomatitis virus. Hum. Gene Ther. **21:**439–450.
18. **Galivo, F., et al.** 2010. Single-cycle viral gene expression, rather than progressive replication and oncolysis, is required for VSV therapy of B16 melanoma. Gene Ther. **17:**158–170.
19. **Gottfried, E., M. Kreutz, and A. Mackensen.** 2008. Tumor-induced modulation of dendritic cell function. Cytokine Growth Factor Rev. **19:**65–77.
20. **Inaba, K., et al.** 2009. Isolation of dendritic cells. Curr. Protoc. Immunol. **3:**3.7.
21. **Kottke, T., et al.** 2011. Broad antigenic coverage induced by vaccination with virus-based cDNA libraries cures established tumors. Nat. Med. **17:**854–859.
22. **Lawson, N. D., E. A. Stillman, M. A. Whitt, and J. K. Rose.** 1995. Recombinant vesicular stomatitis viruses from DNA. Proc. Natl. Acad. Sci. U. S. A. **92:**4477–4481.
23. **Leveille, S., S. Samuel, M. L. Goulet, and J. Hiscott.** 2011. Enhancing VSV oncolytic activity with an improved cytosine deaminase suicide gene strategy. Cancer Gene Ther. **18:**435–443.
24. **Lichty, B. D., A. T. Power, D. F. Stojdl, and J. C. Bell.** 2004. Vesicular stomatitis virus: re-inventing the bullet. Trends Mol. Med. **10:**210–216.
25. **Ludewig, B., et al.** 2000. Induction of optimal anti-viral neutralizing B cell responses by dendritic cells requires transport and release of virus particles in secondary lymphoid organs. Eur. J. Immunol. **30:**185–196.
26. **Maraskovsky, E., et al.** 1996. Dramatic increase in the numbers of functionally mature dendritic cells in Flt3 ligand-treated mice: multiple dendritic cell subpopulations identified. J. Exp. Med. **184:**1953–1962.
27. **Mende, I., and E. G. Engleman.** 2005. Breaking tolerance to tumors with dendritic cell-based immunotherapy. Ann. N. Y. Acad. Sci. **1058:**96–104.
28. **Prestwich, R. J., et al.** 2009. The case of oncolytic viruses versus the immune

system: waiting on the judgment of Solomon. Hum. Gene Ther. **20:**1119–1132.
29. **Randolph, G. J., J. Ochando, and S. Partida-Sanchez.** 2008. Migration of dendritic cell subsets and their precursors. Annu. Rev. Immunol. **26:**293–316.
30. **Rowan, K.** 2010. Oncolytic viruses move forward in clinical trials. J. Natl. Cancer Inst. **102:**590–595.
31. **Shaw, S. G., A. A. Maung, R. J. Steptoe, A. W. Thomson, and N. L. Vujanovic.** 1998. Expansion of functional NK cells in multiple tissue compartments of mice treated with Flt3-ligand: implications for anti-cancer and anti-viral therapy. J. Immunol. **161:**2817–2824.
32. **Steinman, R. M., and J. Banchereau.** 2007. Taking dendritic cells into medicine. Nature **449:**419–426.
33. **Stojdl, D. F., et al.** 2003. VSV strains with defects in their ability to shutdown innate immunity are potent systemic anti-cancer agents. Cancer Cell **4:**263–275.
34. **Willmon, C., et al.** 2011. Vesicular stomatitis virus-induced immune suppressor cells generate antagonism between intratumoral oncolytic virus and cyclophosphamide. Mol. Ther. **19:**140–149.
35. **Willmon, C. L., et al.** 2009. Expression of IFN-beta enhances both efficacy and safety of oncolytic vesicular stomatitis virus for therapy of mesothelioma. Cancer Res. **69:**7713–7720.
36. **Wongthida, P., et al.** 2011. VSV oncolytic virotherapy in the B16 model depends upon intact MyD88 signaling. Mol. Ther. **19:**150–158.
37. **Wongthida, P., et al.** 11 April 2011. Activating systemic T cell immunity against self tumor antigens to support oncolytic virotherapy with vesicular stomatitis virus. Hum. Gene Ther. doi: 10.1089/hum.2010.216.